Effects of Secondary Forces on the Ligand Binding and Conformational State of Antifluorescein Monoclonal Antibody 9-40[†]

Mark E. Mummert and Edward W. Voss, Jr.*

Department of Microbiology, B103 Chemical and Life Sciences Laboratory, University of Illinois, 601 South Goodwin Avenue, Urbana, Illinois 61801-3704

Received September 10, 1996; Revised Manuscript Received July 15, 1997[⊗]

ABSTRACT: Biochemical interactions that occur external to the antibody active site have been termed secondary forces. Secondary forces are supplemental to interactions within the antibody active site (i.e., primary interactions) and can affect ligand binding efficiency as well as variable domain conformation. The antifluorescein antibody system has been determined to be a superior method for delineating primary from secondary interactive components due to the active site-filling properties of the fluorescyl ligand. To date, all studies of secondary forces within the context of the antifluorescein system have been with the high-affinity monoclonal antibody 4-4-20 (mAb 4-4-20) (Mummert & Voss, 1995, 1996, 1997). In order to determine the generality of experimental observations and proposed models, we investigated the effects of secondary forces on the antifluorescein mAb 9-40. In addition to assessing the results of former studies, mAb 9-40 possesses properties unique from those of mAb 4-4-20, namely, a decreased affinity for fluorescein and increased conformational dynamics relative to mAb 4-4-20 (Carrero & Voss, 1996). Results of fluorescein and intrinsic mAb 9-40 tryptophan quenching as well as differential scanning calorimetric (DSC) studies indicated that secondary forces modulated the conformational (metatypic) state in accordance with previous investigations with mAb 4-4-20. Unlike mAb 4-4-20, mAb 9-40 did not exhibit altered ligand binding efficiency due to the inclusion of secondary interactive components. Models were developed that proposed that the increased malleability of mAb 9-40 variable domains could account for functional differences in properties between mAb 9-40 and mAb 4-4-20.

Secondary forces, defined as biochemical interactions external to the classically defined antibody active site, have been shown to affect ligand binding efficiency and conformational properties of the monoclonal antifluorescein antibody 4-4−20 (mAb 4-4-20) (Mummert & Voss, 1995, 1996, 1997). The antifluorescein antibody system is ideal for investigations of secondary forces for a number of reasons: (1) Derivatives of fluorescein (e.g., fluorescein 5-isothiocyanate) are readily available for covalent labeling to a variety of chemically and physically distinct topologies. The effects of these topologies relative to free fluorescein and to each other can be quantitatively evaluated. (2) The fluorescein and the antibody's intrinsic tryptophan fluorescence maximal quenching changes with respect to fluorescein devoid of the carrier matrix and according to the carrier molecule when ligand is bound within the antifluorescein active site (Mummert & Voss, 1995, 1996). (3) The absorptive spectral bathochromic shift of fluorescein changes with respect to fluorescein devoid of the carrier matrix and according to the carrier molecule when the fluorescyl moiety is bound in the antifluorescein active site (Mummert & Voss, 1995, 1996). (4) The kinetic and thermodynamic properties are modulated based on the carrier molecule (Mummert & Voss, 1995, 1996, 1997). (5) The fluorescyl moiety is active site-filling (Voss *et al*., 1976; Herron *et al*., 1989, 1994; Omelyanenko *et al*., 1993; Whitlow *et al*., 1995); therefore, changes in any of the above properties when fluorescein is covalently linked to a carrier must be due to interactions outside of the antibody active site (i.e., secondary forces). Although secondary forces have been evaluated in other systems (vanOss *et al*., 1986), the distinction between primary and secondary interactions has been vague (vanOss, 1995). The site-filling capacity of fluorescein was considered to have negated this confusion (Mummert & Voss, 1995, 1996).

Previous investigations utilizing mAb 4-4-20 with a series of synthetic monofluoresceinated peptides revealed secondary forces decreased the free energy of binding as great as 2 kcal/mol relative to fluorescein devoid of a carrier environment (Mummert & Voss, 1996). Transition-state analyses of various mAb 4-4-20 /monofluoresceinated peptide complexes indicated an enhanced enthalpic activation component relative to fluorescein with no carrier residues. In all cases, enhanced enthalpic activation was offset by an enhanced entropic activation component. The net effect was a decreased energetic barrier for complex decomposition for the monofluoresceinated peptides which resulted in an increased unimolecular rate constant and decreased affinity (Mummert & Voss, 1997).

Analyses of absorptive and fluorescein fluorescence quenching properties of bound monofluoresceinated peptides relative to one another and bound fluorescein devoid of carrier residues indicated distinct changes in these properties relative to their free solution forms. Intrinsic tryptophan fluorescence quenching of mAb 4-4-20 showed distinct but less dramatic changes. These results were collectively interpreted as differences in the final ligand-induced con-

[†] This work was supported by a grant from The American Heart Association, Illinois Affiliate.

* To whom correspondence should be addressed. Phone: (217) 333-0299 or (217) 333-1738. Fax: (217) 244-6697. E-mail: e-voss@uiuc.edu.

[⊗] Abstract published in *Advance ACS Abstracts,* September 15, 1997.

S0006-2960(96)02276-3 CCC: $14.00

formational (metatypic) state. Other evidence has also suggested differential metatypic states as a result of secondary force directed perturbations utilizing anticonformational antibodies (antimetatype antibodies) in a solid phase assay and evaluation of the transmission coefficient (κ) calculated from transition-state analyses (Mummert & Voss, 1996, 1997).

In summary, mAb 4-4-20 and the experiments outlined above have provided quantitative evidence for secondary forces as well as models to interpret experimental results. Secondary forces have been postulated to modulate all of the above parameters via differential metatypic states. The essence of these models held that unliganded (idiotypic) antibody active sites existed in solution as a series of dynamic conformational substates. Upon interacting with homologous ligand, an encounter complex was formed which ultimately led to the final metatypic state. A given metatypic state was envisioned to endow the antibody active site with characteristic spectral and binding properties. Secondary forces were presumed to have modulated the metatypic state (Mummert & Voss, 1995, 1996).

Although studies with mAb 4-4-20 have been useful in elucidating and quantitating secondary forces, other systems should be evaluated in order to determine the generality of the experimental observations and proposed models. Because of the advantages of the antifluorescein system (Voss, 1993), antifluorescyl mAb 9-40 (IgG1, κ) was evaluated utilizing the same monofluoresceinated synthetic peptides utilized with mAb 4-4-20. mAb 9-40 was considered an ideal candidate for a comparison with mAb 4-4-20. First, mAb 9-40 and mAb 4-4-20 are idiotypically but not metatypically related (Bedzyk *et al*., 1986; Voss *et al*., 1988a,b, 1989). Thus, mAb 9-40 is conformationally distinct from mAb 4-4-20. Second, the affinity of mAb 9-40 is ~1000-fold less than mAb 4-4-20 ($\sim 10^7$ M^{-1} as opposed to $\sim 10^{10}$ M^{-1}) (Denzin & Voss, 1992; Bedzyk *et al*., 1986). Thus, secondary force directed perturbations of a moderate affinity antibody could be evaluated. Finally, it has been postulated that the mAb 9-40 variable domains are more dynamic than the mAb 4-4-20 variable domains (Carrero & Voss, 1996). Therefore the effects of dynamics on secondary force directed perturbations could be investigated. Additionally, we hypothesized that differences between idiotypic, metatypic, and secondary force directed metatypic states would be discernible calorimetrically. Other groups have demonstrated that discrete structural states of a protein can be resolved based on differential scanning calorimetry (DSC) (Hiraga & Yutani, 1996; Munson *et al*., 1996). We therefore evaluated these distinct states utilizing DSC.

MATERIALS AND METHODS

Peptide Synthesis. Synthesis of amino-terminal acetylated monofluoresceinated peptides has been described elsewhere (Mummert & Voss, 1996). All peptides used in this study had the following design:

$$\text{Ac-NH-(X)}_6\text{-K-(X)}_6\text{-COO-}$$

where Ac-NH represents the acetylated α-amino group, X represents aspartic, glutamic, or arginine amino acids, and K is the central lysyl residue. Fluorescein 5-isothiocyanate was covalently coupled to the ϵ-amine of the central lysine residue. Purification and verification of syntheses was confirmed as described by Mummert and Voss (1996).

Monoclonal Antibody 9-40. mAb 9-40 was affinity-purified from ascites fluid using a fluorescein−Sepharose 4B column as previously described (Kranz & Voss, 1981; Weidner *et al*., 1993).

Fluorescence Quenching Assays. Fluorescein fluorescence quenching was monitored by titrating a constant concentration of ligand (13.1 nM) with mAb 9-40. Excitation was at 480 nm, and the emission spectra were recorded from 500 to 580 nm. All measurements were performed on a Gregg-PC spectrophotometer (ISS Instruments, Champaign, IL) in 0.1 M phosphate, pH 8.0. Percent quenching was calculated from

$$\% Q = [(A_T - A)/A_T] \times 100 \quad (1)$$

where A_T is the total area under the spectrum in the absence of antibody and A is the area under the spectrum at a given titration. Maximal quenching (Q_{max}) was determined when several additions of antibody did not change the area under the spectrum at that titration.

Intrinsic tryptophan fluorescence quenching was determined by titrating a constant concentration of mAb 9-40 active site (20 nM) with the fluorescein ligands. Excitation was at 280 nm and emission monitored from 320 to 400 nm. All measurements were performed on a Gregg-PC spectrophotometer (ISS Instruments) in 0.1 M phosphate, pH 8.0. Percent quenching was calculated from eq 1 where A_T was the area under the spectrum without the addition of ligand and A is the area under the spectrum at a given ligand concentration. Q_{max} was determined as defined above.

Affinity Determinations. Dissociation constants (K_d) were determined using fluorescence anisotropic methods. mAb 9-40 was serially diluted 1:2 in 0.1 M phosphate, pH 8.0 (1.3 μM starting active site concentration), and the ligand concentration was kept constant (13.1 nM). The total volume for all dilutions was 1.0 mL.

Polarization measurements were conducted with a Gregg-PC spectrophotometer (ISS Instruments) at room temperature. Excitation was at 480 nm and emission monitored through a 510 nm cutoff filter. Anisotropy was calculated from polarization values using $r = 2P/(3 - P)$ where r is anisotropy and P is polarization.

The fractional dissociation was calculated from the following:

$$\alpha = \{1 + Q[(r - r_f)/(r_b - r)]\}^{-1} \quad (2)$$

where α is the fraction dissociated, Q is the ratio of the fluorescence quantum yields in the bound and free forms of ligand, r is the anisotropy at each dilution of mAb 9-40, r_f is the anisotropy of free ligand, and r_b is the anisotropy of totally bound ligand.

The K_d was expressed in the following form:

$$K_d = ([P]_t - [PL])([L]_t - [PL])/[PL] \quad (3)$$

where $[P]_t$ is the total active site concentration, $[L]_t$ is the total ligand concentration, and [PL] is the concentration of the antibody/ligand complex.

Equation 3 was expanded to give the following:

$$[PL]^2 + (K_d - [L]_t - [P]_t)[PL] - ([P]_t - [L]_t) = 0 \quad (4)$$

This was in the form of a quadratic equation ($ax^2 + b - c = 0$) where $a = 1$, $x = [PL]$, $b = K_d - [L]_t - [P]_t$, and $c =$

Table 1: Comparative Quenching of Fluorescein Ligand and Intrinsic Tryptophan Fluorescence upon Binding of FDS and Monofluoresceinated Peptides to mAb 9-40

compound[a]	Q_{max}(F)	Q_{max}(W)
FDS	74.45	72.15
D12KF1	30.56	78.74
E12KF1	53.87	80.90
R12KF1	NQ[b]	72.23
R6D6KF1	22.38	78.83

[a] FDS = fluorescein disodium salt. D12KF1 = monofluoresceinated polyaspartic acid. E12KF1 = monofluoresceinated polyglutamic acid. R12KF1 = monofluoresceinated polyarginine. R6D6KF1 = monofluoresceinated polyarginine/polyaspartic acid. [b] NQ = no quenching.

$[P]_t[L]_t$. By using the quadratic equation with initial estimates of the K_d, [PL] was calculated. Initial estimates of the various K_d values were from Scatchard analyses utilizing tryptophan fluorescence quenching.

The concentration of free active site ($[P]_f$) was determined from the relation:

$$[P]_f = [P]_t - [PL] \quad (5)$$

The fraction dissociated was plotted against log $[P]_f$, and the curves were fit. Curve-fitting resulted in slight deviations of the original estimate of K_d. These new estimates of K_d were then used to recalculate $[P]_f$, and the curves were refitted until the change in the K_d was <1%. All of the described mathematical computations and curve-fitting was accomplished with Delta Graph version 2.0.1. Association constants (K_a) were determined by taking the reciprocal of the K_d.

Differential Scanning Calorimetry (DSC). Approximately 1 mg/mL mAb 9-40 in 0.1 M phosphate, pH 8.0, with and without ligand was used for DSC analyses. Because of the large amount of reagents required for DSC measurements, only one of the monofluoresceinated peptides was used as a model for secondary interactive components. In trials with ligand, 50% of the antibody active sites were filled. Each measurement with protein was preceded by a buffer run with the appropriate ligand to establish the base line. All measurements were performed under nitrogen to avoid boiling and vaporization. The reference cell contained buffer and the appropriate ligand. All measurements were conducted using a MicroCal MC-2 (MicroCal Inc., Northampton, MA) DSC at a scanning rate of 1 K/min. The temperature range was from 25 °C to 90 °C. Thermograms were asymmetric, which was a result of overlapping transitions or scan rate-dependent denaturation. Due to inadequate amounts of material, we were unable to delineate the underlying cause for thermogram asymmetry.

RESULTS

Fluorescence Quenching. Fluorescein fluorescence maximal quenching (i.e., Q_{max}) values were as indicated in Table 1 (Figure 1). The largest value for Q_{max} was with the mAb 9-40/FDS complex (~74%) while the mAb 9-40/R6D6KFl complex indicated no quenching. All Q_{max} values for the remainder of the mAb 9-40/monofluoresceinated peptide complexes showed decreased quenching with respect to mAb 9-40/FDS.

Table 1 also indicates the Q_{max} of the mAb 9-40 intrinsic tryptophan fluorescence. Differences with respect to the mAb 9-40/FDS complex were observed in all cases. All

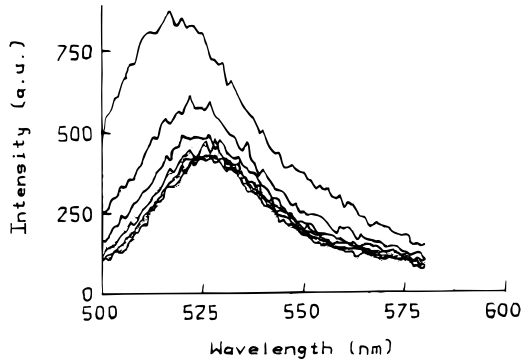

FIGURE 1: Fluorescence quenching was evaluated by monitoring the change in the area of the emission spectra. Maximal quenching was that titration that no longer changed the area under the curve. This is an example of the titration of a monofluoresceinated peptide (E12KFl) with mAb 9-40. Fluorescein emission was monitored from 500 to 580 nm. Intensity had arbitrary units (a.u.).

Table 2: Comparative Association Constants and Changes in Free Energy for the Interaction of FDS and Monfluoresceinated Peptides with mAb 9-40[a]

counpound	K_a[b]	$\Delta G°$ [c]
FDS	$1.00\ (\pm 0.10) \times 10^7$	-9.55 ± 0.06
D12KF1	$6.77\ (\pm 2.02) \times 10^6$	-9.30 ± 0.19
E12LF1	$1.05\ (\pm 0.19) \times 10^7$	-9.57 ± 0.11
R12LF1	$3.09\ (\pm 1.62) \times 10^7$	-10.19 ± 0.31
R6D6KF1	$6.30\ (\pm 3.03) \times 10^6$	-9.23 ± 0.26

[a] All measurements were made in triplicate at 25 °C. [b] K_a = association constant (M^{-1}). [c] $\Delta G°$ = change in free energy of binding (kcal/mol); calculated from $\Delta G° = -RT \ln K_a$.

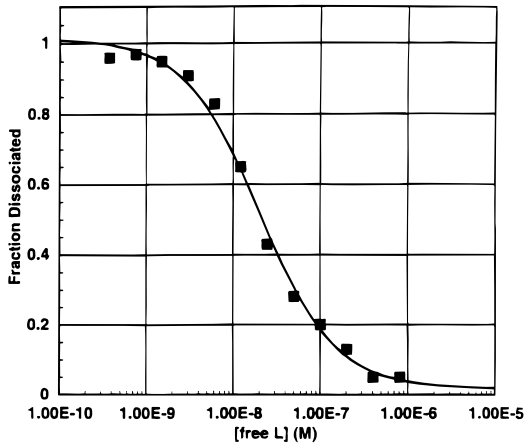

FIGURE 2: Example (R12KFl+9-40) of the quality of the curve-fitting routine using the equations described in the text. Fraction dissociated was calculated from anisotropy, and the concentration of free active site was calculated from a quadratic utilizing an estimated K_d. All calculations and curve-fitting were accomplished with Delta Graph version 2.0.1. Note that plots were semi-logarithmic (Bjerrum plot).

Q_{max} values were enhanced relative to the mAb 9-40/FDS complex except for mAb 9-40/R12KFl which was approximately of the same magnitude.

Association Constants (K_a). Table 2 is a summary of the K_a values determined from fluorescence polarization studies. The free energies of binding were also calculated. All values were statistically indistinguishable ($\sim 1 \times 10^7\ M^{-1}$) as indicated by a *t*-test at the 99% confidence interval. Figure 2 is shown to indicate the quality of data obtained.

Differential Scanning Calorimetry (DSC). Figure 3 indicates the excess heat capacities for the thermal denaturation of the idiotypc and metatypic states of mAb 9-40. Excess

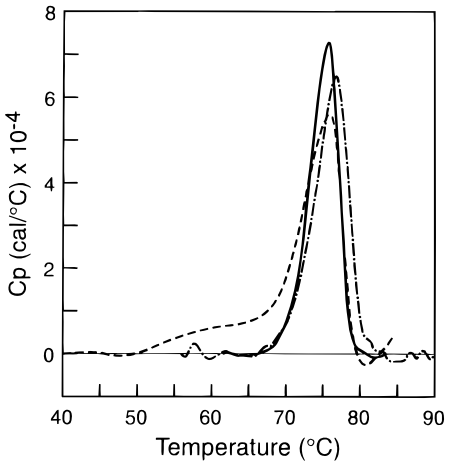

FIGURE 3: Overlay of the excess heat capacity profiles of mAb 9-40 (solid line), mAb 9-40+R12KFl (dashed line), and mAb 9-40+FDS (dashed and dotted line). Excess heat capacity curves were deconvoluted and enthalpic values calculated. Note the shoulder in the mAb 9-40+R12KFl curve which was deconvoluted into an extra peak relative to mAb 9-40 and mAb 9-40+FDS.

heat capacity curves indicated a shoulder for the mAb 9-40+R12KFl complex which was absent from mAb 9-40 and mAb 9-40+FDS.

Specific transition enthalpies (Δh) were determined to be 23.8, 19.6, and 65.1 J/g for mAb 9-40, mAb 9-40+FDS, and mAb 9-40+R12KFl, respectively. The value of 23.8 J/g is in excellent agreement with previous estimations of Δh (24.2 J/g) for IgG1, κ (Buchner *et al*., 1991).

Importantly, pH values were evaluated following all scans. In all cases, it was determined that pH did not change following protein denaturation (i.e., pH 8.0). Therefore, differences in deconvoluted excess heat capacities were assumed not to be due to differences in acidity or alkalinity (Privalov & Potekhin, 1986). When considering DSC analysis, it is important to note that variables such as protein concentration and solvent conditions can modulate quantitative interpretations of thermograms (Tanaka *et al*., 1993). Therefore, results reported herein should be regarded within the confines of the experimental conditions.

DISCUSSION

Secondary interactions have previously been demonstrated to impact the binding and conformational properties of the high-affinity mAb 4-4-20 (Mummert & Voss, 1995, 1996, 1997). In these studies, we have extended the evaluation of secondary interactive components to the moderate affinity mAb 9-40. For reasons described in the introduction, this antibody was considered an ideal candidate. Previous investigations utilized kinetics based on fluorescence quenching to evaluate secondary forces (Mummert & Voss, 1995, 1996, 1997). Low quenching (and in one case no quenching) of the monofluoresceinated peptides and technical limitations in the instrumentation utilized for these experiments prohibited the use of kinetics to evaluate secondary forces on the mAb 9-40/monofluoresceinated complex stabilities.

Previously, mAb 4-4-20 was considered a superior system with which to delineate primary from secondary forces due to the active site-filling properties of the fluorescyl moiety (Herron *et al*., 1989, 1994; Whitlow *et al*., 1995). Bedzyk *et al*. (1990) determined and compared the primary structure of variable heavy (V_H) and variable light (V_L) chains of mAb's 9-40 and 4-4-20. Ten amino acids were different in the V_H chain, all starting with residue H94. Five resided in HCDR3. There were only two amino acid differences in the V_L chain with one non-CDR conserved change (L46) and one significant change in CDR1 (L34). mAb 9-40 was demonstrated to possess the same contact residues as mAb 4-4-20 except for a single substitution ($Arg^{L34} \rightarrow His^{L34}$). Although the X-ray crystal structure of mAb 9-40 has yet to be determined, it has been inferred from molecular modeling studies that fluorescein is also a site-filling moiety as in mAb 4-4-20 (Omelyanenko *et al*., 1993). In the following discussion, we have assumed that secondary forces were a result of interactions between the environment of the fluorescyl moiety and regions surrounding the mouth of the mAb 9-40 active site.

Results of fluorescein and mAb 9-40 intrinsic tryptophan quenching when the fluorescyl moiety resided in the antibody active site indicated significant differences in these values relative to fluorescein devoid of carrier residues and relative to one another (Table 1). Similar results have been reported for mAb 4-4-20 with identical monofluoresceinated peptides (Mummert & Voss, 1996). Changes in quenching have been interpreted as differences in the metatypic state (Mummert & Voss, 1995, 1996). The basic models that have been developed assume that antibody variable domains exist as a series of conformational states (i.e., idiotypic states) (Voss *et al*., 1988a,b, 1992). Homologous ligand selects the most energetically favorable idiotypic state (conformer selection), and upon binding homologous ligand, an encounter complex is formed. The encounter complex undergoes a conformational change that results in the final thermally averaged metatypic state (Voss, 1993). Distinct metatypic states have characteristic quenching properties. Inclusion of secondary interactions resulted in perturbations of the metatypic state and thus modulated the characteristic quenching properties of the antifluorescein antibody. Thus, the observation that secondary forces resulted in modulation of the quenching properties of mAb 9-40 inferred that interactions between regions surrounding the mouth of the active site and residues of the peptide carriers modulated the conformation of the antibody variable domains. This observation and hypothesis was consistent with results of the impact of secondary forces on mAb 4-4-20 (Mummert & Voss, 1995, 1996).

Evaluation of the association constants and free energies of binding indicated that there was no statistical basis to differentiate between the various mAb 9-40 complexes (Table 2). In contrast, these same monofluoresceinated peptides resulted in marked modulations of the mAb 4-4-20 association constants and free energies of binding (Mummert & Voss, 1996). Apparently, mAb 9-40 was able to compensate for the secondary forces in the free energy of binding. Carrero and Voss (1996) postulated that the mAb 9-40 variable domains have greater dynamics than mAb 4-4-20 as inferred by experiments with hydrostatic pressure. Assumedly, the greater dynamics of the mAb 9-40 variable domains result in greater conformational degrees of freedom. The net result of this conformational latitude is apparently the ability of mAb 9-40 to interact with a wider array of chemical environments without sacrificing the free energy of binding. It has been previously demonstrated that mAb 9-40 is a highly cross-reactive antibody (Carrero & Voss, 1996). Thus, unlike the high affinity and relatively more rigid mAb 4-4-20 molecule, mAb 9-40 is able to compensate for secondary effects much more efficiently in terms of the

free energy of binding. Presumably, this is a result of the conformational freedom of the mAb 9-40 variable domains. These results indicated that secondary forces modulated the metatypic state (as evidenced by fluorescence quenching results) without significantly affecting the free energy of binding.

Results of DSC analyses indicated the thermal denaturation of idiotypic and metatypic mAb 9-40 (Figure 3). Metatypic mAb 9-40 without secondary interactive (i.e., mAb 9-40+FDS) components showed the same thermal denaturation pattern as idiotypic mAb 9-40. This result indicated that both conformers of the molecule had equivalent thermal stability. We hypothesized that the extra peak was partly attributable to differences in bond formation due to secondary interactions between residues of the carrier peptide and regions surrounding the mouth of the antibody active site. This interpretation was supported by Δh values which provided an estimation of the number and/or strength of intramolecular bonds (Buchner *et al*., 1991). The larger value of Δh (65.1 J/g) for the mAb 9-40+R12KFl complex relative to mAb 9-40+FDS ($\Delta h = 19.6$ J/g) and mAb 9-40 ($\Delta h = 24.2$ J/g) was interpreted to be a result of increased intramolecular bond formation due to secondary forces. We hypothesized that the decreased value of Δh (19.6 J/g) for mAb 9-40+FDS was consistent with displaced solvent due to ligand binding. Secondary forces are a result of various noncovalent interactions (Mummert & Voss, 1997). Differences in thermal sensitivity and specific transition enthalpy were postulated to be due to the metatypic state induced by secondary forces (e.g., atomic packing and/or hydration). Calorimetric analyses were therefore postulated to be a sensitive indicator of conformation.

Buchner *et al*. (1991) demonstrated that the folded state of an immunoglobulin affects Δh and thermal denaturation. We hypothesized that the conformational state also impacted Δh and thermal denaturation. From these results, we concluded that the mAb 9-40+FDS complex was structurally more similar (although definitely not identical) to idiotypic mAb 9-40 than the mAb 9-40/R12KFl complex. Secondary forces therefore resulted in conformations that were perturbed to a greater extent than the metatypic state devoid of secondary forces relative to idiotypic mAb 9-40.

In conclusion, we have examined the effects of secondary forces on the primary interaction of a moderate affinity, dynamic antifluorescein antibody. Results of quenching indicated that secondary forces perturbed the metatypic state relative to ligand binding in the absence of carrier residues. This perturbation, however, had no effect on the free energy of ligand binding as evidenced by anisotropy studies. We proposed that the increased malleability of the mAb 9-40 variable domains reconciled these results. It is tempting to speculate a relationship exists between low- to moderate-affinity antibodies and enhanced dynamics relative to high-affinity antibodies. Such a relationship has been proposed by others (Padlan, 1994). Results of DSC indicated differences in metatypic and idiotypic states. Further differences were observed for metatypic states with and without secondary forces. These differences in Δh values and thermal sensitivity were hypothesized to be due to differences in the various conformational states. Such differences may have been due to differences in atomic packing and/or levels of hydration that existed for the different conformational states. This work reinforces the generality of previous work with the high-affinity antifluorescein mAb 4-4-20 (Mummert & Voss, 1995, 1996, 1997) that secondary forces play a role in dictating conformational states.

ACKNOWLEDGMENT

All quenching and polarization experiments were conducted at the Laboratory for Fluorescence Dynamics (University of Illinois, Urbana−Champaign). We thank Drs. Jenny Carrero and Theodore Hazlett for their insight and stimulating conversations.

REFERENCES

Bedzyk, W. D., Reinitz, D. M., & Voss, E. W., Jr. (1986) *Mol. Immunol. 23*, 1319−1328.
Bedzyk, W. D., Herron, J. N., Edmundson, A. B., & Voss, E. W., Jr. (1990) *J. Biol. Chem. 265*, 133−138.
Buchner, J., Renner, M., Lilie, H., Hinz, H.-J., Jaenicke, R., Kiefhaber, T., & Rudolph, R. (1991) *Biochemistry 30*, 6922−6929.
Carrero, J., & Voss, E. W., Jr. (1996) *J. Biol. Chem. 271*, 5332−5337.
Denzin, L. K., & Voss, E. W., Jr. (1992) *J. Biol. Chem. 267*, 8925−8931.
Herron, J. N., He, X., Mason, M. L., Voss, E. W., Jr., & Edmundson, A. B. (1989) *Proteins: Struct., Funct., Genet. 5*, 271−280.
Herron, J. N., Johnston, T. S., He, X., Guddat, L., Voss, E. W., Jr., & Herron, A. B. (1994) *Biophys. J. 67*, 2167−2183.
Hiraga, K., & Yutani, K. (1996) *Protein Eng. 9*, 425−431.
Kranz, D. M., & Voss, E. W., Jr. (1981) *J. Biol. Chem. 257*, 6987−6995.
Mummert, M. E., & Voss, E. W., Jr. (1995) *Mol. Immunol. 32*, 1225−1233.
Mummert, M. E., & Voss, E. W., Jr. (1996) *Biochemistry 35*, 8187−8192.
Mummert, M. E., & Voss, E. W., Jr. (1997) *Mol. Immunol. 33*, 1067−1077.
Munson, M., Balasubramanian, S., Fleming, K. G., Nagi, A. D., O'Brien, R., Sturtevant, J. M., & Regan, L. (1996) *Protein Sci. 5*, 1584−1593.
Omelyanenko, V. G., Jiskoot, W., & Herron, J. N. (1993) *Biochemistry 32*, 10423−10429.
Padlan, E. A. (1994) *Mol. Immunol. 31*, 169−217.
Privalov, P. L., & Potekhin, S. A. (1986) *Methods Enzymol. 131*, 5−51.
Tanaka, A., Flanagan, J., & Sturtevant, J. M. (1993) *Protein Sci. 2*, 567−576.
vanOss, C. J. (1995) *Mol. Immunol. 32*, 199−211.
vanOss, C. J., Good, R. J., & Chaudhury, M. K. (1986) *J. Chromatogr. 376*, 111−119.
Voss, E. W., Jr. (1993) *J. Mol. Recognit. 6*, 51−58.
Voss, E. W., Jr., Eschenfeldt, W., & Root, R. T. (1976) *Immunochemistry 12*, 745−749.
Voss, E. W., Jr., Dombrink-Kurtzman, M. A., & Miklasz, S. D. (1988a) *Immunol. Invest. 17*, 25−39.
Voss, E. W., Jr., Miklasz, S., Petrossian, A., & Dombrink-Kurtzman, M. A. (1988b) *Mol. Immunol. 25*, 751−759.
Voss, E. W., Jr., Dombrink-Kurtzman, M. A., & Ballard, D. W. (1989) *Mol. Immunol. 26*, 971−977.
Voss, E. W., Jr., Weidner, K. M., & Denzin, L. K. (1992) *Immunol. Invest. 21*, 71−83.
Weidner, K. M., Denzin, L. K., Kim, M. L., Mallender, W. D., Miklasz, S. D., & Voss, E. W., Jr. (1993) *Mol. Immunol. 30*, 1003−1011.
Whitlow, M., Howard, A. J., Wood, J. F., Voss, E. W., Jr., & Hardman, K. D. (1995) *Protein Eng. 8*, 749−761.

BI962276I